

Direct determination of optimal real-space orbitals for correlated electronic structure of molecules.

Edward F. Valeev,^{*,†} Robert J. Harrison,[‡] Charles C. Peterson,[¶] and Deborah A. Penchoff[§]

[†]*Department of Chemistry, Virginia Tech, Blacksburg, VA 24061*

[‡]*Department of Applied Mathematics & Statistics, Stony Brook University, Stony Brook, NY 11794*

[¶]*Office of Advanced Research Computing, University of California, Los Angeles, CA 90095*

[§]*UT Innovative Computing Laboratory, University of Tennessee, Knoxville, TN 37996*

E-mail: efv@vt.edu

July 25, 2022

Abstract

We demonstrate how to determine nearly numerically exact orthonormal orbitals that are optimal for evaluation of the energy of arbitrary (correlated) states of atoms and molecules by minimization of the energy Lagrangian. Orbitals are expressed in real space using multiresolution spectral element basis that is refined adaptively to achieve the user-specified target precision while avoiding the ill-conditioning issues that plague AO basis set expansions traditionally used for correlated models of molecular electronic structure. For light atoms the orbital solver in conjunction with a variational electronic structure model [selected Configuration Interaction (CI)] provides energies of

comparable precision to a state-of-the-art atomic CI solver. The computed electronic energies of atoms and molecules are significantly more accurate than the counterparts obtained with the Gaussian AO bases of the same rank, and can be determined even when linear dependence issues preclude the use of the AO bases.

1 Introduction

Predictive computation of properties of molecules and materials requires highly-*accurate* treatment of many-electron correlation effects as well as *precise* numerical representation of the many-body states and operators involved therein. In molecular and, increasingly, in solid-state contexts many-body methods have utilized the Linear Combination of Atomic Orbitals (LCAO) numerical representation of 1-particle (orbital) states constructed from pre-optimized sequences of atom-centered basis sets (represented by analytic Gaussian-type or Slater-type functions, or represented numerically¹). However, (augmented) plane-wave (PW) representation of 1-particle states can also be used.² Unfortunately representation of many-particle by products of 1-particle states suffers from slow convergence in the vicinity of electron cusps,³ thereby mandating the use of basis set extrapolation⁴ or the augmentation with explicit 2-particle basis (“explicit correlation”).⁵⁻⁸

Although the LCAO-based many-body methods can be pushed match experimental thermochemical⁹ and spectroscopic data¹⁰ for small molecules, extending such successes to increasingly larger systems, and to higher accuracy, is limited by the rapid onset of ill-conditioning, high-order rise of operator evaluation with the AO angular momenta, and the challenges of fast (reduced-scaling) reformulation of such methods due to the increasing density of the representation in the high-precision regime. LCAO representation in practice is a heavily empirical endeavour: at this moment the Basis Set Exchange reference database¹¹ lists 402 Gaussian AO basis sets designed for representing orbitals of a carbon atom. Albeit the large number of officially-recognized bases is simply due to the long history of the Gaussian AO technology, many recently-designed bases have rather niche uses; navigating

the basis set zoo is a near-expert task, especially when treating high-density solids¹² or computing properties other than the energy.¹³ Meanwhile plane wave representation struggles with description of localized features (e.g., atomic shell structure, nuclear cusps and Coulomb holes) of the electronic wave functions and thus are not naturally suitable to compact and/or fast formulations.

An attractive alternative to the LCAO and PW representations for many-body electronic structure are *real-space* numerical representations, a loosely-defined group including finite difference (FD), which only use grids and lack explicit basis functions, and finite element (FE) and spectral element (SE) methods, which utilize basis functions with strictly local support. Such representations combine the ability to resolve short and long lengthscale features of the many-body electronic wave functions with promise of systematic bias-free improvability without ill-conditioning issues. Due to these favorable features there has been a flurry of activity in developing real-space numerical technology for fast 1-body methods, such as Kohn-Sham density functional theory.

Unfortunately the use of real-space representation has been far more limited for many-body methods applicable to general molecules due to the exponential growth of the representation of a k -particle state with k . Even methods like MP2 and CCSD in real-space formulation involve representation of 2-particle wave operators (hence, 6-dimensional functions); while for atoms pair theories have been explored for a relatively long time,¹⁴⁻¹⁷ for molecules the feasibility of such representations has been demonstrated only recently by some of us (MP2)^{18,19} and our collaborators (CIS(D), CC2)^{20,21} by combining volume-element-wise pair function compression and R12/F12-style regularization of electron cusps.¹⁸ It is possible to obtain energies and properties with such methods that are competitive to the state-of-the-art LCAO technology for small polyatomics, but the methodology is still relatively limited and likely cannot be made practical 3- and higher-body methods.

A more practical alternative to the direct real-space representation of 2-particle states is to expand them in products of real-space orbitals. Although such approaches, unlike

the direct many-body representations, suffer from the slow convergence near electron cusps, the same remedies as used for the LCAO-based many-body methods (namely, the basis set extrapolation or R12/F12-style explicit correlation) can be deployed to fix these shortcomings. In the purely orbital-based many-body framework the key differences between spectral (LCAO, PW) and real-space representations is limited to the orbital optimization and evaluation of the physical operators. Due to the cost of both in the real-space representation real-space many-body methods have been implemented for atoms (both at the multiconfiguration self-consistent field (MCSCF)²²⁻²⁴ and perturbative levels²⁵) and diatomic molecules (MCSCF,^{24,26,27} perturbation theory²⁸ and coupled-cluster (CC)^{29,30}); an excellent recent review of the vast relevant literature by Lehtola can be found in Ref. 31.

The first demonstration of any real-space orbital-based many-body method applicable to general molecules was shown recently by Kottmann, Bischoff, and Valeev.³² The key to this advance was the realization that far more compact orbital representation of the weakly-occupied (virtual) orbitals needed for dynamical correlation is provided by the pair-natural orbitals.³³⁻³⁵ The PNO-MP2-F12 method using the real-space representation for all orbitals was demonstrated for molecules with more than 30 atoms, with precision surpassing what is achievable by the state-of-the-art LCAO technology.

While the work showed a viable roadmap for developing many-body perturbation theory (MBPT) and related methods with real-space orbitals, a single Slater determinant often does not provide a qualitatively correct starting point. In this paper we ask whether it is possible

1. to express arbitrary (not just MBPT-based) orbital-based many-body wave functions in terms of real-space orbitals, and
2. robustly determine optimal design for such orbitals.

We conclude that the answer to these questions is affirmative.

The rest of the paper is organized as follows. Section 2 describes the correlated multiresolution orbital solver. Section 3 describes the technical details of the computational

experiments that are reported and analyzed in Section 4. Section 5 summarizes our findings and outlines future directions.

2 Formalism

Consider the energy functional of a (unit-normalized) state Ψ in a Fock-space state defined by M (spin-)orbitals $\{\phi_p\}$:

$$E(|\Psi\rangle) = \langle\Psi|\hat{H}|\Psi\rangle = \gamma_i^j h_j^i + \frac{1}{2}\gamma_{ij}^{kl} g_{kl}^{ij}, \quad (1)$$

where γ_j^i and γ_{kl}^{ij} are the (spin-orbital) 1- and 2-RDMs (see Appendix A for the notation and standard definitions). For a fixed *model* defining the map from orbitals $\{\phi_p\}$ to $|\Psi\rangle$, Eq. (1) defines a functional of the orbitals. Our objective is to minimize this functional with respect to M *orthonormal* orbitals $\{\phi_p\}$. Unlike the traditional approaches, such as (MC)SCF, in which the orbitals are typically represented as a linear combination of a fixed basis [e.g., an atomic orbital basis in the linear-combination-of-atomic-orbitals (LCAO) formalism] in this work each orbital is expressed in a basis adaptively refined to approach the orbital’s exact representation in the full Hilbert space.

To enforce the orbital orthonormality we introduce a Lagrangian,

$$L = \langle\Psi|\hat{H}|\Psi\rangle - \epsilon_j^i (s_i^j - \delta_i^j). \quad (2)$$

Variation $\phi_m^* \rightarrow \phi_m^* + \delta$ produces the following first-order change in the Lagrangian:

$$\left\langle \frac{\partial L}{\partial \phi_m^*} \right\rangle = 2 \left(\gamma_i^m \hat{h} + \gamma_{ij}^{mk} \hat{g}_k^j - \epsilon_i^m \right) |\phi_i\rangle \quad (3)$$

The optimal orbitals are determined by solving

$$\left| \frac{\partial L}{\partial \phi_m^*} \right\rangle \stackrel{\text{opt}}{=} 0 \quad (4)$$

The multipliers are determined by projecting Eq. (4) onto the current (orthonormal) orbitals:

$$\left\langle \phi_n \left| \frac{\partial L}{\partial \phi_m^*} \right. \right\rangle = 2 (\gamma_i^m h_n^i + \gamma_{ij}^{mk} g_{nk}^{ij} - \epsilon_n^m) = 0, \quad \text{or} \quad (5)$$

$$\epsilon_n^m = \gamma_i^m h_n^i + \gamma_{ij}^{mk} g_{nk}^{ij}. \quad (6)$$

This choice of the multipliers makes the gradient automatically orthogonal to the current orbitals.

If $|\Psi\rangle$ is a single Slater determinant (SD) (e.g., a Hartree-Fock determinant) the RDMs simplify,

$$\gamma_j^i \stackrel{\text{SD}}{=} \delta_j^i, \quad (7)$$

$$\gamma_{kl}^{ij} \stackrel{\text{SD}}{=} \delta_k^i \delta_l^j - \delta_l^i \delta_k^j, \quad (8)$$

and the gradient becomes:

$$\left| \frac{\partial L}{\partial \phi_m^*} \right\rangle \stackrel{\text{SD}}{=} 2 (\hat{f} |\phi_m\rangle - f_i^m |\phi_i\rangle). \quad (9)$$

Its projection onto an arbitrary orbital ϕ_a orthogonal to all current orbitals is

$$\left\langle \phi_a \left| \frac{\partial L}{\partial \phi_m^*} \right. \right\rangle \stackrel{\text{SD}}{=} 2 f_a^m, \quad (10)$$

vanishing of which with the optimal orbitals is the Brillouin condition.

For multiconfigurational states Eqs. (3) and (6) for the Lagrangian gradient and multipliers take the SD-like form when the 2-RDM is rewritten in terms of its cumulant (see

Appendix A). This nominally results in replacements $h \rightarrow f$, $\gamma \rightarrow \lambda$:

$$\left\langle \frac{\partial L}{\partial \phi_m^*} \right\rangle = 2 \left(\gamma_i^m \hat{f} + \lambda_{ij}^{mk} \hat{g}_k^j - \epsilon_i^m \right) |\phi_i\rangle, \quad (11)$$

$$\epsilon_n^m = \gamma_i^m f_n^i + \lambda_{ij}^{mk} g_{nk}^{ij}. \quad (12)$$

Clearly, Eq. (9) follows from Eq. (11) due to the vanishing 2-RDM cumulant for the SD state.

The use of *natural* orbitals (NOs), which make the 1-RDM diagonal,

$$\gamma_n^m \stackrel{\text{NO}}{=} \begin{cases} \gamma_m^m, & m = n \\ 0, & m \neq n \end{cases} \quad (13)$$

further simplifies the gradient and makes possible to design a simple orbital update strategy similar to that used for SD³⁶ and correlating orbitals³² in a real-space representation:

$$\left\langle \frac{\partial L}{\partial \phi_m^*} \right\rangle \stackrel{\text{NO}}{=} 2 \left(\gamma_m^m \hat{f} |\phi_m\rangle + (\lambda_{ij}^{mk} \hat{g}_k^j - \epsilon_i^m) |\phi_i\rangle \right). \quad (14)$$

Partitioning the Fock operator \hat{f} into its free-particle component \hat{d} (the kinetic energy in the nonrelativistic case, or the Dirac operator in the relativistic case) and the rest \hat{v} , the orbital stationarity condition becomes:

$$- \left(\hat{d} - \tilde{\epsilon}_m \right) |\phi_m\rangle = \hat{v} |\phi_m\rangle + \frac{1}{\gamma_m} \left(\gamma_{ij}^{mk} \hat{g}_k^j |\phi_i\rangle - \sum_{i \neq m} \epsilon_i^m |\phi_i\rangle \right), \quad (15)$$

where

$$\tilde{\epsilon}_m \equiv \frac{\epsilon_m^m}{\gamma_m} \stackrel{\text{NO}}{=} f_m^m + \sum_{ijk} \frac{\lambda_{ij}^{mk} g_{mk}^{ij}}{\gamma_m} = h_m^m + \sum_{ijk} \frac{\gamma_{ij}^{mk} g_{mk}^{ij}}{\gamma_m} \quad (16)$$

is the effective energy of NO m . The orbital update described below exploits the fact

that $\tilde{\epsilon}_m < 0$ for all orbitals, even weakly occupied. To understand why that is consider the following decomposition of the electronic energy (Eq. (1)) into the contributions from natural orbital m and the rest:

$$E \equiv E_m + E_{-m}$$

$$E_m \equiv 2 \operatorname{Re} \left(\gamma_m^m h_m^m + \sum_{ijk} \gamma_{ij}^{km} g_{km}^{ij} \right) = 2 \operatorname{Re} \epsilon_m^m. \quad (17)$$

Since the electronic energy cannot decrease in magnitude as the orbital basis is expanded, E_m approximates the absolute decrease in the energy due to the exclusion of orbital m from the orbital set, hence this is why ϵ_m^m is nonnegative.

Updated orbitals are obtained by the action of Green's operator of particle in constant potential $-\tilde{\epsilon}_m > 0$ on the r.h.s. of Eq. (15):

$$|\phi_m\rangle = -\hat{G}_{-\tilde{\epsilon}_m} \left(\hat{v} |\phi_m\rangle + \frac{1}{\gamma_m^m} \left(\lambda_{ij}^{mk} \hat{g}_k^j |\phi_i\rangle - \sum_{i \neq m} \epsilon_i^m |\phi_i\rangle \right) \right). \quad (18)$$

For a nonrelativistic particle and open boundary conditions Green's operator has the familiar Yukawa kernel:

$$x > 0 : \hat{G}_{-x} f(\mathbf{r}) = -2 \int \frac{\exp(-\sqrt{2x}|\mathbf{r} - \mathbf{r}'|)}{4\pi|\mathbf{r} - \mathbf{r}'|} f(\mathbf{r}') d\mathbf{r}' \quad (19)$$

extensions to the periodic boundary conditions³⁷ and Dirac particles³⁸ are also known.

The rate of convergence of Eq. (18) is rapid, but it is possible to accelerate it further by extrapolation. To this end we deploy the Krylov-subspace Accelerated Inexact Newton (KAIN) method;³⁹ other strategies like BFGS⁴⁰ should be usable as well. Note that to be able to make KAIN extrapolation robust it is essential to choose a canonical frame for the orbitals.

It is useful to point out how Eq. (18) is related to the orbital update used to determine optimal single-determinant orbitals in Ref. 36. For a single determinant the cumulant

vanishes and

$$\epsilon_n^m \stackrel{\text{SD}}{=} f_n^m. \tag{20}$$

Since the SD energy is invariant with respect to orbital rotations, the orbital update Eq. (18) can be optimally simplified by switching to the *canonical* orbitals that diagonalize the Lagrangian coefficients ϵ (i.e., the Fock matrix in this case):

$$|\phi_m\rangle \stackrel{\text{SD}}{=} -\hat{G}_{-\epsilon_m} \hat{v} |\phi_m\rangle, \tag{21}$$

which coincides with the orbital update used in Ref. 36.

3 Technical Details

The orbital solver has been implemented in a developmental version of the Massively Parallel Quantum Chemistry (MPQC) package⁴¹ using the implementation of the MRA calculus in the MADNESS library.⁴² The solver is bootstrapped with Gaussian AOs taken from the user-provided basis and projected onto the spectral element basis. RDMs were obtained from 1- and 2-electron integrals evaluated in the spectral element basis using a Heat-Bath CI (HCI)⁴³ solver developed in MPQC. All atomic calculations and the minimal basis H₁₀ benchmark set HCI selection thresholds $\epsilon_{1,2}$ to zero; the H₁₀ computation bootstrapped from the cc-pVDZ basis used $\epsilon_{\{1,2\}} = 10^{\{-4,-6\}}$.

Despite using the efficient production-grade implementation of the MRA calculus in MADNESS, the current implementation is not fully optimal. Although optimization of 100 or more correlated (i.e., with nonzero cumulant contributions) orbitals is feasible with the current (CPU-only) code, the implementation of the time-determining step in the orbital update, namely the 2-cumulant-dependent contribution to Eq. (18), does not explicitly optimize for CPU caches and can be significantly improved (by one to two orders of magnitude)

even without exploiting accelerators. Thus in this initial report we limited computations to 50 correlated orbitals for which an orbital update step takes < 3 hours on a single 32-core node.

4 Results

4.1 Atoms

4.1.1 He

The CI energies obtained with fixed Gaussian AO bases and the corresponding spectral-element orbitals obtained therefrom are shown in Table 1.

Unsurprisingly, the use of optimized numerical orbitals results in significant lowerings of the CI energy. Clearly, orbital optimization alone only addresses the suboptimality of the given orbital set of a fixed finite rank (“orbital error”, quantified by $E_{\text{AO}} - E_{\text{MRA}}$); the basis set incompleteness due to the finite rank (“rank error”, quantified by $E_{\text{MRA}} - E_{\text{exact}}$) is not addressed by the orbital optimization and requires increasing the rank (ideally, in conjunction with extrapolation or explicit correlation). Nevertheless, it is somewhat surprising how substantial is the the orbital errors of the correlation consistent basis sets (that are optimized for atomic CI energies⁴⁴) relative to their rank errors, shown in the second-to-last column in Table 1. Even for a quadruple-zeta basis orbital relaxation lowers the energy by 60% of the residual basis set error. These findings are in line with the unexpected sensitivity of the CC singles and doubles energy to the details of the unoccupied (pair-natural) orbitals that we found in the LCAO context.⁴⁵

What is more surprising, however, is that usually significant ($> 50\%$) fraction of the energy lowering due to the orbital optimization can be attributed to the relaxation of the weakly-occupied (correlating) orbitals. To estimate this fraction the last column shows the the energy lowering due to relaxing the occupied Hartree-Fock (1s) orbital from its finite

basis form to the exact form, as a percentage of the total CI energy lowering due to the orbital optimization. For example, with the cc-pVTZ AO basis only 33 % of the CI energy lowering can be attributed to the basis set incompleteness of the Hartree-Fock occupied orbital; this is somewhat unexpected considering that the correlation consistent basis family was optimized for atomic CI computations. This finding emphasizes that even numerical deficiencies of even weakly occupied orbitals can contribute significantly to the overall basis set errors of correlated energies.

Table 1: Converged CI energies (mE_h) of the ground-state He atom evaluated with Gaussian AO and optimized MRA orbitals. The exact energy is $-2903.724 mE_h$. The energies are converged to all digits shown.

Basis ^a	AO		MRA		AO vs MRA	
	E_{AO}	$E_{AO} - E_{\text{exact}}$	E_{MRA}	$E_{MRA} - E_{\text{exact}}$	$\frac{E_{AO} - E_{MRA}}{E_{MRA} - E_{\text{exact}}} \times 100\%$	$\frac{E_{AO}^{\text{HF}} - E_{\text{exact}}^{\text{HF}}}{E_{AO} - E_{MRA}} \times 100\%$
1s	-2 846.292	57.43	-2 861.679	42.05	37	100
2s1p	-2 887.595	16.13	-2 897.674	6.05	167	64
3s2p1d	-2 900.232	3.49	-2 901.840	1.88	86	33
4s3p2d1f	-2 902.411	1.31	-2 902.909	0.82	61	34
5s4p3d2f1g	-2 903.152	0.57	-2 903.297	0.43	35	40

^a Gaussian computations used the standard STO-6G and cc-pVD,T,Q,5Z basis sets, respectively. MRA orbitals were obtained by optimization starting from the Gaussian AO basis sets.

As Figure 1 illustrates, the changes in the natural orbitals due to the basis set relaxation can indeed be significant, not only near the nucleus (where Gaussian orbitals lack the cusp) and far from the nucleus (where Gaussians decay too quickly) but also at the intermediate distances from the nucleus where the orbital magnitude and positions of the radial nodes can be strongly impacted by the orbital optimization.

As illustrated in Table 2, the orbital solver can robustly optimize orbital sets with occupancies differing by many orders of magnitude. As elaborated in Section 2, the effective orbital energy, $\tilde{\epsilon}$, that controls the orbital update via the Greens function (Eq. (18)) is negative even for the weakly-occupied NOs; in fact, they are even more negative than the energy of the strongly occupied NO. In contrast, the corresponding diagonal elements of the Fock operator are positive, as expected. The difference between the Fock and effective orbital energies is negligible for the strongly occupied NO.

Table 2: Properties of the leading natural orbitals for the He ground state obtained from the cc-pVTZ basis.

ϕ_p	γ_p^p	F_p^p, E_h	$\tilde{\epsilon}_p^p, E_h$
1s	1.984	-0.913	-0.958
2s	7.69×10^{-3}	1.595	-2.935
2p	2.60×10^{-3}	2.058	-3.305
3s	1.08×10^{-4}	7.400	-8.319
3p	7.05×10^{-5}	7.879	-8.789
3d	5.85×10^{-5}	5.927	-6.997

4.2 Be

For the ground state of Be the energy lowering due to the orbital relaxation was similar to what was found for He (see Table Table 3. Microhartree-level agreement was found with the atomic CI solver in the state-of-the-art GRASP package.⁴⁶

Table 3: Converged CI energies (mE_h) of the ground-state He atom evaluated with Gaussian AO (“LCAO”), optimized real-space orbitals (“MRA”), and the atomic finite-difference MCSCF solver in the GRASP2K software (“FD”).⁴⁶ The LCAO and MRA energies are converged to all digits shown.

Basis	LCAO	MRA	FD
2s1p	-14.556 089	-14.616 856	-14.616 854
3s2p1d	-14.617 410	-14.654 415	-14.654 406
4s3p2d1f	-14.623 808	-14.661 475	-14.661 478
complete	-14.667 354 7 ^a		

^a Ref. 47.

4.3 Molecules

4.4 H₁₀

We chose H₁₀ in its ground state as a model system for testing solver robustness due to the availability of extensive benchmarks for a number of methods.⁴⁸ The system offers the ability to control the nature and strength of electron correlation by varying the interatomic distance and the size of the orbital basis. In particular, at short interatomic distances (R) even the smallest nonminimal (double-zeta) Gaussian AO basis becomes nearly linearly dependent and

accurate evaluation of the Hamiltonian and the method-specific iterative solvers can become untenable. At short R the importance of angular correlation greatly increases compared to the equilibrium and stretched R . Lastly, the use of a minimal AO basis (1 orbital per atom) maximizes the degree of “on-site” repulsion and increases the extent of longitudinal correlation.

The initial investigation of our orbital solver focused on the maximally-compressed geometry considered in Ref. 48, where achieving the basis set limit with the standard Gaussian basis sets is difficult due to the rapid onset of ill-conditioning, which recently motivated developments of mixed numerical representations marrying Gaussian AOs with real-space approaches.⁴⁹ As expected, the orbital optimization greatly reduces the basis set incompleteness of the CI energy, as can be seen in the rightmost column of Table 4, by $\times 3.4$ for the STO-6G basis and by $\times 7.4$ for the cc-pVDZ basis. The estimated residual basis set error with the MRA-optimized cc-pVDZ orbitals is $< 3mE_h$ / atom; this is already comparable to the $1mE_h$ uncertainty in the estimated nonrelativistic energy at this distance.⁴⁸

Table 4: Converged CI energies (E_h) of the equidistant 10-atom chain of H atoms at compressed geometry (interatomic separation of 1 a.u.; see Ref. 48 for more details) evaluated with Gaussian AOs (“LCAO”) and optimized real-space orbitals (“MRA”), as well as the ratio of the respective basis set errors.

Basis	LCAO	MRA	$\Delta_{\text{LCAO}}/\Delta_{\text{MRA}}$
STO-6G	-3.824 4	-4.251 5	3.4
cc-pVDZ	-4.219 5	-4.400 3	7.4
complete	-4.428 4 ^a		

^a AFQMC value from Ref. 48.

Figure 2 contains the plots of the frontier natural orbitals (counterparts of the HOMO and LUMO Hartree-Fock orbitals). The qualitative structures of the LCAO and real-space NOs are similar: both exhibit the same number of nodes and the same symmetry with respect to the inversion center. As expected, and just like in the atoms, the real-space NOs exhibit correct nuclear cusps and slower asymptotic decay into the vacuum. Interestingly, however, real-space NOs have lower probability densities at most nuclei than their Gaussian

counterparts.

5 Summary

We presented a general method for constructing orbitals that are optimal for computing energies with correlated (many-body methods) in arbitrary molecules and with robust control of numerical errors. In this work we employed multiresolution adaptive discontinuous spectral-element representation for the orbitals, but the presented method can be used with other real-space representations. Although utilized with the conventional and selected configuration interaction wave functions, the orbital solver can be used with arbitrary maps from orbitals to 1- and 2-particle reduced density matrices (e.g., tensor networks, stochastic methods, or quantum circuits). Numerical performance of the method was demonstrated by computing the CI energies of small atoms (matching the numerical precision of the atomic finite-difference CI codes) and a paradigmatic compressed polyatomic molecule; in all cases the use of real-space representation for the orbitals yielded energies that were significantly lower than the Gaussian AO-based counterparts, with correct asymptotic behavior at the nuclei and in vacuum.

Further algorithmic improvements should allow to speed up the rate determining steps in the orbital updates by 1 or 2 orders of magnitude even without employing accelerated hardware (such as general-purpose graphical processing units). The formalism should also map straightforwardly to the optimization of molecular spinors for relativistic correlated methods by borrowing the advances in 4-component relativistic numerical electronic structure introduced by some of us recently.³⁸ Work along these lines is already underway and will be reported elsewhere.

Acknowledgement

This work was supported by the U.S. Department of Energy via award DE-SC0022327. EFV

is grateful to Greg Beylkin for providing the quadratures described in Ref. 50.

Appendix A Notation and Standard Definitions

In this work we largely follow a covariant tensor notation of the many-body quantum chemistry.^{51,52} Einstein summation convention is implied, unless sums over any index are shown explicitly: namely, summation is implied over every symbol that appears once in a *contravariant* (upper, bra) position and once as in a *covariant* (lower, ket) position in a given tensor *product*, with the summation range defined by the symbol.

Matrix elements of one-, two-, and higher-body operators are denoted as follows:

$$\langle p | \hat{o}(1) | q \rangle \equiv \int \phi_p^*(1) \hat{o}(1) \phi_q(1) d1 \equiv o_p^q \quad (22)$$

$$\langle p_1 p_2 | \hat{o}(1, 2) | q_1 q_2 \rangle \equiv \int \phi_{p_1}^*(1) \phi_{p_2}^*(2) \hat{o}(1, 2) \phi_{q_1}(1) \phi_{q_2}(2) d1 d2 \equiv o_{p_1 p_2}^{q_1 q_2}, \text{ etc.} \quad (23)$$

It is convenient to use similar notation for one- and higher-body functions resulting from omission of one or more bra indices (and the corresponding integrations) in the matrix elements:

$$\hat{o}(1) \phi_q(1) \equiv \hat{o} | \phi_q \rangle \equiv o_{\perp}^q, \quad (24)$$

$$\left(\int \phi_{p_2}^*(2) \hat{o}(1, 2) \phi_{q_2}(2) d2 \right) \phi_{q_1}(1) \equiv \hat{o}_{p_2}^{q_2} | \phi_{q_1} \rangle \equiv o_{\perp p_2}^{q_1 q_2}, \quad \text{etc.} \quad (25)$$

All many-body operators in this manuscript are particle-symmetric, i.e. $o(1, 2) = o(2, 1)$, hence $o_{q_1 q_2}^{p_1 p_2} = o_{q_2 q_1}^{p_2 p_1}$. Matrix elements of the 1- and 2-particle parts of the Hamiltonian are denoted by h_q^p and g_{rs}^{pq} , respectively.

$$f_q^p \equiv h_q^p + (g_{qs}^{pr} - g_{sq}^{pr}) \gamma_r^s, \quad (26)$$

where γ_r^s denotes elements of 1-RDM (see Eq. (29)), are the familiar matrix elements of the

Fock operator. The overlap of two functions is denoted by s_q^p . δ_q^p denotes the Kronecker delta:

$$\delta_q^p = \begin{cases} 1, & p = q \\ 0, & p \neq q \end{cases} \quad (27)$$

2- and 1-RDMs for state $|\Psi\rangle$ are defined as:

$$\gamma_{kl}^{ij} \equiv \langle \Psi | \hat{a}_i^\dagger \hat{a}_j^\dagger \hat{a}_l \hat{a}_k | \Psi \rangle, \quad (28)$$

$$\gamma_j^i \equiv \langle \Psi | \hat{a}_i^\dagger \hat{a}_j | \Psi \rangle \equiv \frac{2}{N-1} \sum_k \gamma_{ik}^{jk}, \quad (29)$$

with \hat{a}_i^\dagger and \hat{a}_i the standard creators and annihilators, respectively. If $|\Psi\rangle$ is a multideterminantal/multiconfiguration (MC) state it is convenient to represent 2-RDM as

$$\gamma_{kl}^{ij} \equiv \gamma_k^i \gamma_l^j - \gamma_l^i \gamma_k^j + \lambda_{kl}^{ij}, \quad (30)$$

with λ_{kl}^{ij} the 2-RDM *cumulant*.⁵³

Appendix B Spherical projection of orbital updates

In atomic computations it is useful to be able to obtain solutions with specific target number of subshells, e.g. 3s2p1d for a second-row atom. In general such solutions are saddle points; tracking such saddle points can fail if the gradient does not preserve the relevant symmetries exactly. Unfortunately the finite-precision spectral element bases employed in this work do not preserve spherical symmetry. Thus we need to impose symmetry restrictions on the orbital updates; without such restrictions the solutions may break spherical symmetry.

Consider a subshell of $2l + 1$ “noisy” orbitals. To project out the components of the orbitals corresponding to other angular momenta we want to express each atomic orbital as

a product of its radial component $f(r)$ times the angular factor, i.e. as

$$\phi_i(\mathbf{r}) \approx f(r) \sum_m^{2l+1} u_i^m Y_{lm}(\theta, \phi), \quad (31)$$

where the angular component is written as a unitary linear combination of spherical harmonics to support arbitrary orientation of each orbital. We determine $f(r)$ by minimizing the average deviation of the subshell orbitals:

$$\Delta \equiv \sum_i^{2l+1} \left\| \phi_i(\mathbf{r}) - f(r) \sum_m^{2l+1} u_i^m Y_{lm}(\theta, \phi) \right\|_2. \quad (32)$$

The gradient with respect to f is:

$$\begin{aligned} \frac{\delta \Delta}{\delta f} &= 2 \sum_i^{2l+1} \left\langle \phi_i - f \sum_m^{2l+1} u_i^m Y_{lm} \left| \sum_{m'}^{2l+1} u_i^{m'} Y_{lm'} \right. \right\rangle \\ &= 2 \sum_{m'}^{2l+1} u_i^{m'} \sum_i^{2l+1} \langle \phi_i | Y_{lm'} \rangle - 2f \sum_i^{2l+1} \sum_m^{2l+1} u_i^m \sum_{m'}^{2l+1} u_i^{m'} \delta_{m'}^m \\ &= 2 \sum_{m'}^{2l+1} u_i^{m'} \sum_i^{2l+1} \langle \phi_i | Y_{lm'} \rangle - (4l + 2)f \end{aligned} \quad (33)$$

This suggests the following formula for f for the given fixed coefficients u :

$$f = \frac{1}{2l+1} \sum_{m'}^{2l+1} u_i^{m'} \sum_i^{2l+1} \langle \phi_i | Y_{lm'} \rangle. \quad (34)$$

To determine nearly-optimal values of coefficients u for a given subshell orbital i we evaluate its overlaps with the spherical harmonics $S_{m,g}^{(i)} \equiv \langle \phi_i | Y_{lm} \rangle (r_g)$ on a uniform radial grid $\{r_g = g\delta_r, \forall g = 1..n_g\}$. Here we set the grid size n_g to 10 and the grid extent $\delta_g(n_g + 1)$ to $\sqrt{\frac{2\pi^2}{T_i}}$, which is the de Broglie wavelength of a free particle with kinetic energy $T_i \equiv \langle \phi_i | \hat{T} | \phi_i \rangle$. Note that these kinetic energies are available since detection of orbital subshells also used their kinetic energies. Coefficients $u_i^{m'}$ are given by the left-hand singular vector corresponding to the largest singular value of $(\mathbf{S}^{(i)})_{m,g} \equiv S_{m,g}$. Angular integration is performed via the

lowest-order (72 points) rotationally invariant quadratures of Ahrens and Beylkin.⁵⁰

References

- (1) Blum, V.; Gehrke, R.; Hanke, F.; Havu, P.; Havu, V.; Ren, X.; Reuter, K.; Scheffler, M. Ab Initio Molecular Simulations with Numeric Atom-Centered Orbitals. *Comput. Phys. Commun.* **2009**, *180*, 2175–2196.
- (2) Schäfer, T.; Ramberger, B.; Kresse, G. Quartic Scaling MP2 for Solids: A Highly Parallelized Algorithm in the Plane Wave Basis. *J. Chem. Phys.* **2017**, *146*, 104101.
- (3) Kato, T. On the Eigenfunctions of Many-particle Systems in Quantum Mechanics. *Commun. Pure Appl. Math.* **1957**, *10*, 151–177.
- (4) Helgaker, T.; Klopper, W.; Koch, H. Basis-Set Convergence of Correlated Calculations on Water. *J. Chem. Phys.* **1997**, *106*, 9639–9646.
- (5) Klopper, W.; Manby, F. R.; Ten-no, S.; Valeev, E. F. R12 Methods in Explicitly Correlated Molecular Electronic Structure Theory. *Int. Rev. Phys. Chem.* **2006**, *25*, 427–468.
- (6) Kong, L.; Bischoff, F. A.; Valeev, E. F. Explicitly Correlated R12/F12 Methods for Electronic Structure. *Chem. Rev.* **2012**, *112*, 75–107.
- (7) Hättig, C.; Klopper, W.; Köhn, A.; Tew, D. P. Explicitly Correlated Electrons in Molecules. *Chem. Rev.* **2012**, *112*, 4–74.
- (8) Grüneis, A.; Shepherd, J. J.; Alavi, A.; Tew, D. P.; Booth, G. H. Explicitly Correlated Plane Waves: Accelerating Convergence in Periodic Wavefunction Expansions. *J. Chem. Phys.* **2013**, *139*, 084112.
- (9) Tajti, A.; Szalay, P. G.; Császár, A. G.; Kállay, M.; Gauss, J.; Valeev, E. F.; Flowers, B. A.; Vázquez, J.; Stanton, J. F. HEAT: High Accuracy Extrapolated Ab Initio Thermochemistry. *J. Chem. Phys.* **2004**, *121*, 11599–11613.

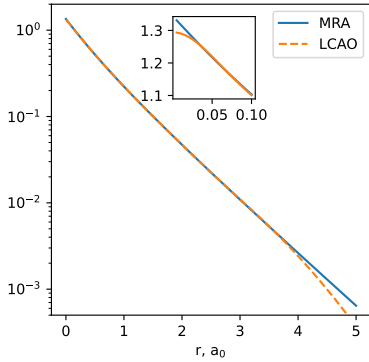
- (10) Barletta, P.; Shirin, S. V.; Zobov, N. F.; Polyansky, O. L.; Tennyson, J.; Valeev, E. F.; Császár, A. G. CVRQD Ab Initio Ground-State Adiabatic Potential Energy Surfaces for the Water Molecule. *J. Chem. Phys.* **2006**, *125*, 204307.
- (11) Pritchard, B. P.; Altarawy, D.; Didier, B.; Gibson, T. D.; Windus, T. L. New Basis Set Exchange: An Open, Up-to-Date Resource for the Molecular Sciences Community. *J. Chem. Inf. Model.* **2019**, *59*, 4814–4820.
- (12) VandeVondele, J.; Hutter, J. Gaussian Basis Sets for Accurate Calculations on Molecular Systems in Gas and Condensed Phases. *J. Chem. Phys.* **2007**, *127*, 114105.
- (13) Baranowska, A.; Sadlej, A. J. Polarized Basis Sets for Accurate Calculations of Static and Dynamic Electric Properties of Molecules. *J. Comput. Chem.* **2009**, NA–NA.
- (14) Flores, J. R. High Precision Atomic Computations from Finite Element Techniques: Second-order Correlation Energies of Rare Gas Atoms. *J. Chem. Phys.* **1993**, *98*, 5642–5647.
- (15) Ackermann, J. Finite-Element-Method Expectation Values for Correlated Two-Electron Wave Functions. *Phys. Rev. A* **1995**, *52*, 1968–1975.
- (16) Flores, J. R.; Kolb, D. Atomic MP2 Correlation Energies Fast and Accurately Calculated by FEM Extrapolations. *J. Phys. B At. Mol. Opt. Phys.* **1999**, *32*, 779.
- (17) Flores, J. R. New Benchmarks for the Second-Order Correlation Energies of Ne and Ar through the Finite Element MP2 Method: Second-Order Correlation Energies of Ne and Ar. *Int. J. Quantum Chem.* **2008**, *108*, 2172–2177.
- (18) Bischoff, F. A.; Harrison, R. J.; Valeev, E. F. Computing Many-Body Wave Functions with Guaranteed Precision: The First-Order Møller-Plesset Wave Function for the Ground State of Helium Atom. *J. Chem. Phys.* **2012**, *137*, 104103.

- (19) Bischoff, F. A.; Valeev, E. F. Computing Molecular Correlation Energies with Guaranteed Precision. *J. Chem. Phys.* **2013**, *139*, 114106.
- (20) Kottmann, J. S.; Bischoff, F. A. Coupled-Cluster in Real Space. 1. CC2 Ground State Energies Using Multiresolution Analysis. *J. Chem. Theory Comput.* **2017**, *13*, 5945–5955.
- (21) Kottmann, J. S.; Bischoff, F. A. Coupled-Cluster in Real Space. 2. CC2 Excited States Using Multiresolution Analysis. *J. Chem. Theory Comput.* **2017**, *13*, 5956–5965.
- (22) Fischer, C. F. Superposition of Configuration Results for SI II. *ApJ* **1968**, *151*, 759.
- (23) Fischer, C. F. Average-Energy-of-Configuration Hartree-Fock Results for the Atoms Helium to Radon Charlotte Froese Fischer. *Atomic Data and Nuclear Data Tables* **1972**, *4*, 301–399.
- (24) Sundholm, D.; Olsen, J.; Malmqvist, P.-Å.; Roos, B. O. In *Numerical Determination of the Electronic Structure of Atoms, Diatomic and Polyatomic Molecules*; DeFranceschi, M., Delhalle, J., Eds.; Springer Netherlands: Dordrecht, 1989; pp 329–334.
- (25) Dzuba, V. A.; Flambaum, V. V.; Kozlov, M. G. Combination of the Many-Body Perturbation Theory with the Configuration-Interaction Method. *Phys. Rev. A* **1996**, *54*, 3948–3959.
- (26) Adamowicz, L.; McCullough, E. A. A Numerical Multiconfiguration Self-consistent-field Method for Diatomic Molecules. *J. Chem. Phys.* **1981**, *75*, 2475–2476.
- (27) Laaksonen, L.; Sundholm, D.; Pyykkö, P. Two-Dimensional Fully Numerical MC SCF Calculations on H₂ and LiH: The Dipole Moment of LiH. *Chemical Physics Letters* **1984**, *105*, 573–576.
- (28) McCullough, E. A.; Morrison, J.; Richman, K. W. Numerical Perturbation Calculations for Diatomic Molecules. *Faraday Symp. Chem. Soc.* **1984**, *19*, 165.

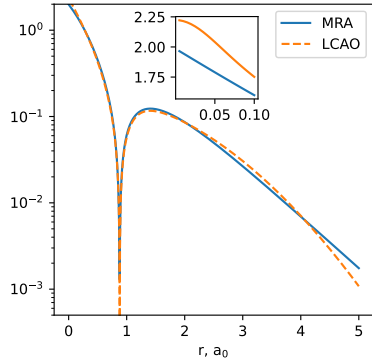
- (29) Adamowicz, L.; Bartlett, R. J. Coupled Cluster Calculations with Numerical Orbitals for Excited States of Polar Anions. *J. Chem. Phys.* **1985**, *83*, 6268–6274.
- (30) Adamowicz, L.; Bartlett, R. J.; McCullough, E. A. Towards Numerical Solutions of the Schrödinger Equation for Diatomic Molecules. *Phys. Rev. Lett.* **1985**, *54*, 426–429.
- (31) Lehtola, S. A Review on Non-relativistic, Fully Numerical Electronic Structure Calculations on Atoms and Diatomic Molecules. *Int J Quantum Chem* **2019**, *119*.
- (32) Kottmann, J. S.; Bischoff, F. A.; Valeev, E. F. Direct Determination of Optimal Pair-Natural Orbitals in a Real-Space Representation: The Second-Order Moller–Plesset Energy. *J. Chem. Phys.* **2020**, *152*, 074105.
- (33) Edmiston, C.; Krauss, M. Configuration-Interaction Calculation of H₃ and H₂. *J. Chem. Phys.* **1965**, *42*, 1119–1120.
- (34) Meyer, W. Ionization Energies of Water from PNO-CI Calculations. *Int. J. Quantum Chem.* **1971**, *5*, 341–348.
- (35) Neese, F.; Hansen, A.; Liakos, D. G. Efficient and Accurate Approximations to the Local Coupled Cluster Singles Doubles Method Using a Truncated Pair Natural Orbital Basis. *J. Chem. Phys.* **2009**, *131*, 064103.
- (36) Harrison, R. J.; Fann, G. I.; Yanai, T.; Gan, Z.; Beylkin, G. Multiresolution Quantum Chemistry: Basic Theory and Initial Applications. *J. Chem. Phys.* **2004**, *121*, 11587–11598.
- (37) Jia, J.; Hill, J. C.; Beylkin, G.; Harrison, R. J. MULTIREOLUTION FAST METHODS FOR A PERIODIC 3-D NAVIER-STOKES SOLVER. Proceedings of the 8th International Symposium on Distributed Computing and Applications to Business, Engineering and Science. 2009; pp 13–16.

- (38) Anderson, J.; Sundahl, B.; Harrison, R.; Beylkin, G. Dirac-Fock Calculations on Molecules in an Adaptive Multiwavelet Basis. *J. Chem. Phys.* **2019**, *151*, 234112.
- (39) Harrison, R. J. Krylov Subspace Accelerated Inexact Newton Method for Linear and Nonlinear Equations. *J. Comput. Chem.* **2004**, *25*, 328–334.
- (40) Yao, Y.; Umrigar, C. J. Orbital Optimization in Selected Configuration Interaction Methods. *J. Chem. Theory Comput.* **2021**, *17*, 4183–4194.
- (41) Peng, C.; Lewis, C. A.; Wang, X.; Clement, M. C.; Pierce, K.; Rishi, V.; Pavošević, F.; Slattery, S.; Zhang, J.; Teke, N.; Kumar, A.; Masteran, C.; Asadchev, A.; Calvin, J. A.; Valeev, E. F. Massively Parallel Quantum Chemistry: A High-Performance Research Platform for Electronic Structure. *J. Chem. Phys.* **2020**, *153*, 044120.
- (42) Harrison, R. J.; Beylkin, G.; Bischoff, F. A.; Calvin, J. A.; Fann, G. I.; Fosso-Tande, J.; Galindo, D.; Hammond, J. R.; Hartman-Baker, R.; Hill, J. C.; Jia, J.; Kottmann, J. S.; Yvonne Ou, M.-J.; Pei, J.; Ratcliff, L. E.; Reuter, M. G.; Richie-Halford, A. C.; Romero, N. A.; Sekino, H.; Shelton, W. A.; Sundahl, B. E.; Thornton, W. S.; Valeev, E. F.; Vázquez-Mayagoitia, Á.; Vence, N.; Yanai, T.; Yokoi, Y. MADNESS: A Multiresolution, Adaptive Numerical Environment for Scientific Simulation. *SIAM J. Sci. Comput.* **2016**, *38*, S123–S142.
- (43) Holmes, A. A.; Tubman, N. M.; Umrigar, C. J. Heat-Bath Configuration Interaction: An Efficient Selected Configuration Interaction Algorithm Inspired by Heat-Bath Sampling. *J. Chem. Theory Comput.* **2016**, *12*, 3674–3680.
- (44) Dunning, T. H. Gaussian Basis Sets for Use in Correlated Molecular Calculations. I. The Atoms Boron through Neon and Hydrogen. *J. Chem. Phys.* **1989**, *90*, 1007–1023.
- (45) Clement, M. C.; Zhang, J.; Lewis, C. A.; Yang, C.; Valeev, E. F. Optimized Pair Natural Orbitals for the Coupled Cluster Methods. *J. Chem. Theory Comput.* **2018**, *14*, 4581–4589.

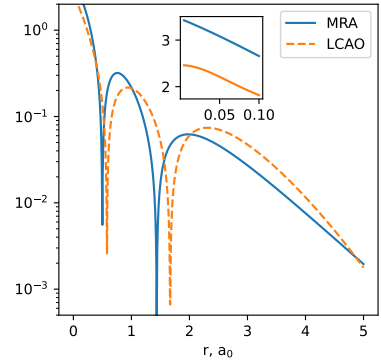
- (46) Jönsson, P.; Gaigalas, G.; Bieroń, J.; Fischer, C. F.; Grant, I. New Version: Grasp2K Relativistic Atomic Structure Package. *Computer Physics Communications* **2013**, *184*, 2197–2203.
- (47) Sims, J. S.; Hagstrom, S. A. Hylleraas-Configuration-Interaction Study of the 1 S Ground State of Neutral Beryllium. *Phys. Rev. A* **2011**, *83*, 032518.
- (48) Motta, M.; Ceperley, D. M.; Chan, G. K.-L.; Gomez, J. A.; Gull, E.; Guo, S.; Jiménez-Hoyos, C. A.; Lan, T. N.; Li, J.; Ma, F.; Millis, A. J.; Prokof'ev, N. V.; Ray, U.; Scuseria, G. E.; Sorella, S.; Stoudenmire, E. M.; Sun, Q.; Tupitsyn, I. S.; White, S. R.; Zgid, D.; Zhang, S.; Simons Collaboration on the Many-Electron Problem, Towards the Solution of the Many-Electron Problem in Real Materials: Equation of State of the Hydrogen Chain with State-of-the-Art Many-Body Methods. *Phys. Rev. X* **2017**, *7*, 1.
- (49) Stoudenmire, E. M.; White, S. R. Sliced Basis Density Matrix Renormalization Group for Electronic Structure. *Phys. Rev. Lett.* **2017**, *119*, 046401.
- (50) Ahrens, C.; Beylkin, G. Rotationally Invariant Quadratures for the Sphere. *Proc. R. Soc. A.* **2009**, *465*, 3103–3125.
- (51) Harris, F. E.; Jeziorski, B.; Monkhorst, H. J. Contraction Theorem for the Algebraic Reduction of (Anti)Commutators Involving Operator Strings. *Phys. Rev. A* **1981**, *23*, 1632–1638.
- (52) Kutzelnigg, W. Quantum Chemistry in Fock Space. I. The Universal Wave and Energy Operators. *J. Chem. Phys.* **1982**, *77*, 3081–3097.
- (53) Kutzelnigg, W.; Mukherjee, D. Cumulant Expansion of the Reduced Density Matrices. *J. Chem. Phys.* **1999**, *110*, 2800–2809.



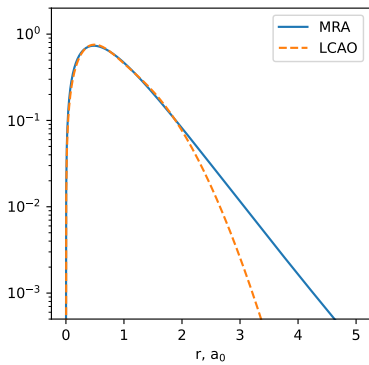
(a) 1st $l = 0$ NO



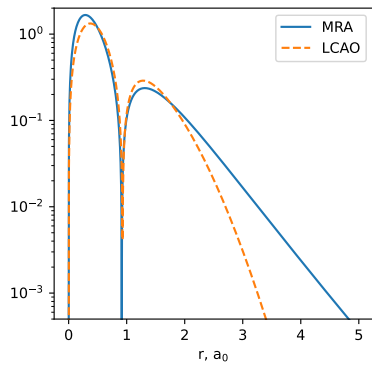
(b) 2nd $l = 0$ NO



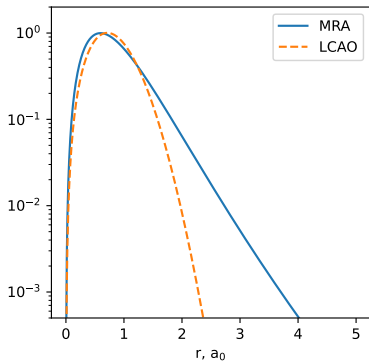
(c) 3rd $l = 0$ NO



(d) 1st $l = 1$ NO

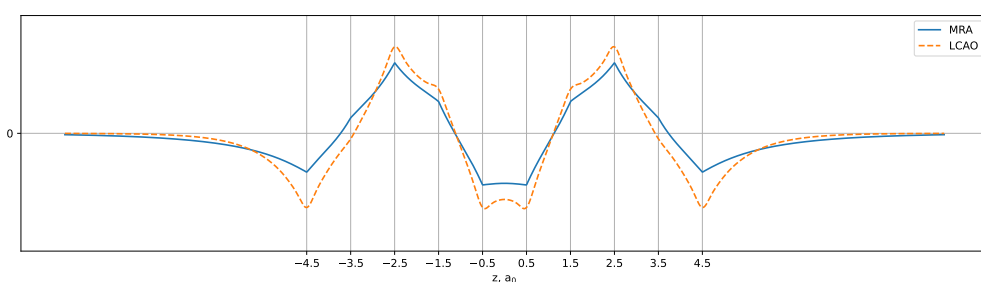


(e) 2nd $l = 1$ NO

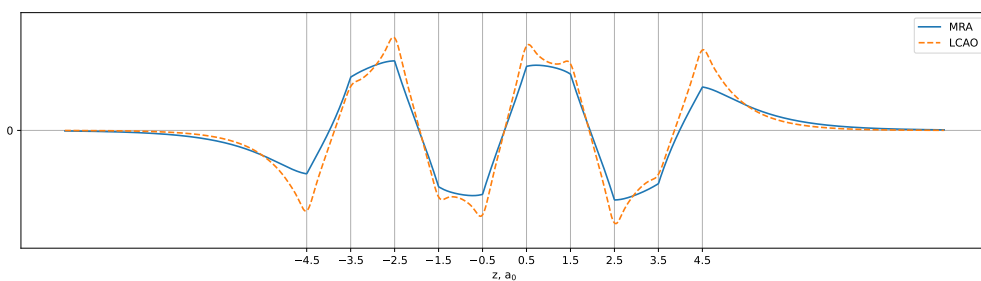


(f) 1st $l = 2$ NO

Figure 1: Comparison of 6 largest-occupancy NOs of the ground-state He atom evaluated using Gaussian cc-pVTZ basis (“LCAO”) and the real-space orbitals (“MRA”) obtained therefrom. Gaussian-based NOs decay too rapidly in the asymptotic limit as well as fail to reproduce the cusp at the nucleus for the $l = 0$ case.



(a) 5th NO



(b) 6th NO

Figure 2: Plots of frontier NOs of H_{10} evaluated with STO-6G Gaussian AOs (“LCAO”) and the corresponding optimized real-space orbitals (“MRA”) along the molecular axis.